Master's thesis

NTNU
Norwegian University of Science and Technology
Faculty of Information Technology and Electrical Engineering
Department of Mathematical Sciences

Peder Eggen Skaug

Numerical Estimates for Point Evaluation in Paley–Wiener Spaces

Master's thesis in Applied Physics and Mathematics
Supervisor: Kristian Seip
June 2024

NTNU
Norwegian University of
Science and Technology

Peder Eggen Skaug

Numerical Estimates for Point Evaluation in Paley–Wiener Spaces

Master's thesis in Applied Physics and Mathematics
Supervisor: Kristian Seip
June 2024

Norwegian University of Science and Technology
Faculty of Information Technology and Electrical Engineering
Department of Mathematical Sciences

ABSTRACT

This master's thesis studies a problem on time-frequency localization, namely that of computing the norm of point evaluation in Paley–Wiener L^p spaces, denoted PW^p, with emphasis on the range $1 < p < 2$. We have sought upper and lower bounds using methods based on theoretical and numerical techniques developed in the paper *An Extension of Bohr's Inequality* by Lars Hörmander and Bo Bernhardsson, who studied the case $p = 1$. We have produced lower bounds through a numerical implementation of the Newton–Raphson method, and will present evidence supporting that the upper bound is not much larger than these lower bounds.

SAMMENDRAG

Denne masteroppgaven studerer et problem innen tid-frekvens lokalisering, nemlig å beregne normen av punkt-evaluering i såkalte Paley–Wiener L^p rom, der $1 < p < 2$. Vi har forsøkt å finne nedre og øvre grenser ved hjelp av metoder basert på teoretiske og numeriske teknikker utviklet i artikkelen *An Extension of Bohr's Inequality* av Lars Hörmander og Bo Bernhardsson, som studerte tilfellet $p = 1$. Vi har produsert nedre begrensninger ved å implementere en Newton–Raphson metode, og vil presentere resultater som støtter at de øvre begrensningene ikke er mye større enn de nedre.

PREFACE

This master's thesis marks the culmination of my journey through the master's program in Applied Physics and Mathematics at NTNU. It has been 5 years of intense learning, both academically and personally, and I am deeply grateful for the opportunities and support I have received along the way. I am also grateful for the opportunity to delve into the world of time-frequency analysis, and to immerse myself in a single topic for an entire semester.

First and foremost I would like to thank my supervisor, Kristian Seip, for his invaluable guidance and encouragement over the past year. Your expertise and insights have been crucial to the development of this thesis. I would also like to thank my classmates, for countless hours of struggles, but also for countless lunch breaks, table tennis matches, and walks around campus.

Last, but not least, I want to thank my family, for their unwavering love, support, and encouragement throughout my studies. I dedicate this thesis to you.

Peder Eggen Skaug
June 2024, Trondheim.

CONTENTS

LIST OF FIGURES

LIST OF TABLES

ABBREVIATIONS

List of abbreviations, in alphabetical order;

- **a.e.** Almost everywhere
- **e.g.** Exempli gratia, "for example"
- **i.e.** Id est, "that is"
- **SDG** Sustainable Development Goals

CHAPTER

ONE

INTRODUCTION

1.1 Project description

We are studying the following problem in time-frequency localization; what is the smallest constant C, called $\mathscr{C}_p$, such that the inequality

$$|f(0)|^p \leq C||f||_p^p \tag{1.1.1}$$

holds for all f in PW^p, where $1 < p < 2$?

1.2 Motivation

In time-frequency analysis, one of the classic problems is that of estimating point-evaluation, especially in spaces of integrable functions, such as PW^p, where one generally does not have pointwise control. The main motivation for this thesis is that lower and upper bounds for $\mathscr{C}_p$ have been furnished for all other convex PW^p spaces, that is $2 < p < \infty$, see [1]. Therefore it is of interest to see whether such explicit bounds can be found for $1 < p < 2$. The thesis also attempts to directly answer problem 4 in the survey of Lubinsky [2].

The problem is also interesting in the context of uncertainty principles, as uncertainty principles in Fourier analysis describe the interplay between the decay of a function and the smoothness of its Fourier transform.

1.3 Outline of the thesis

The main idea of the thesis is to attempt to utilise and modify the techniques from Hörmander and Bernhardsson's paper *An extension of Bohr's inequality* [3] to produce upper and lower estimates for $\mathscr{C}_p$ for $1 < p < 2$. The lower estimates were found by solving an extremal problem in L^p numerically. The upper estimates were considerably harder to produce, as Hörmander's analysis for the upper estimate of $\mathscr{C}_1$ does not naturally extend to PW^p for $1 < p < 2$. Evidence supporting the upper bounds being close to the lower bounds, however, will be presented. In the end we will present and discuss some results for estimates of $\mathscr{C}_p$, and discuss what further improvements can be made.

1.4 Sustainability

As part of the thesis, it is mandatory that we discuss the thesis' relevance to the United Nations SDGs. Mathematical research, like this thesis, contributes to increasing the body of knowledge used in higher education, something which fall under **Goal 4: Quality education**.

Mathematical research is also a fundamental part of technological innovation. Breakthroughs in time-frequency localization can have applications in fields such as signal analysis or telecommunication, or other technologies that are essential to modern infrastructure. This fits well with **Goal 9: Industry, Innovation and Infrastructure**.

Other than these goals, it is hard to find some concrete relevance to the SDGs, mainly because this thesis is a purely theoretical one, and is without any immediate real-life applications at this point in time.

CHAPTER

TWO

PRELIMINARIES

The Paley–Wiener spaces PW^p are the subspaces of $L^p(\mathbb{R})$ consisting of functions f that are entire and of exponential type at most π. We denote by $||\cdot||_p$ the standard L^p-norm on the real line, that is

$$||f||_p = \left(\int_{-\infty}^{\infty} |f(x)|^p dx \right)^{1/p}.$$

Similarly, we will call $||f||_p^p$ the L^p **integral** of f. A function is said to be of exponential type if its growth is bounded by an exponential $e^{A|z|}$ for large $|z|$, that is there exists some finite constant $C = C(A)$ such that

$$|f(z)| \leq Ce^{A|z|} \quad \text{as} \quad |z| \to \infty.$$

Its type is then the infimum of all such A's. Since any function in PW^p is both entire and of exponential type $\leq \pi$, by the Paley–Wiener theorem [4, Theorem 4], its Fourier transform is supported in $[-\pi, \pi]$. We will throughout the thesis be using the following normalization of the Fourier transform and its corresponding inverse transform;

$$\widehat{f}(\xi) = \int_{-\infty}^{\infty} f(x)e^{-ix\xi}dx, \quad f(x) = \frac{1}{2\pi}\int_{-\infty}^{\infty} \widehat{f}(\xi)e^{ix\xi}d\xi.$$

It is assumed that the reader has some knowledge of introductory Fourier analysis, functional analysis and L^p-theory.

What is interesting, is the behaviour of (1.1.1) as an uncertainty principle. As mentioned in the introduction, an uncertainty principle describes the interplay between the decay of a function, and the smoothness of its Fourier transform. This is the same as saying f and $\widehat{f}$ cannot both be localized on small sets. This is nicely illustrated by the Fourier transform of the delta measure, $\delta(x)$, which, in the sense of distributions, is

$$\widehat{\delta} = 1,$$

which is completely delocalized, while the delta measure itself is sharply localized. In layman's terms one could say the Fourier transform "spreads out" sharply localized signals. In L^p spaces, as $p \searrow 0$, $f \in L^p$ needs to be increasingly rapidly decaying. An L^1-integrable function may blow up near 0, but must decay rapidly

enough as $|x| \to \infty$, while an L^∞ function need not decay at all, but cannot blow up. Rapid decay of f means $\widehat{f}$ needs to be increasingly smooth as $p \searrow 0$. Since, in PW^p, $\operatorname{supp} \widehat{f} \subset [-\pi, \pi]$, this imposes a limit on how large the Fourier transform can grow on $[-\pi, \pi]$ without losing smoothness. Since we have the following relation

$$f(0) = \int_{-\pi}^{\pi} \widehat{f}(\xi) \frac{d\xi}{2\pi},$$

(1.1.1) can be interpreted as an uncertainty principle on PW^p, describing the relation between the decay of f and its blow-up at the origin.

The case $p = 1$ was studied by Lars Hörmander and Bo Bernhardsson in their paper *An extension of Bohr's Inequality* [3], which was published in 1993. The project thesis was devoted to studying this paper, and also reproducing the numerical results [5]. In their paper, Hörmander and Bernhardsson were able to find numerical estimates for $\mathscr{C}_1$,

$$0.5409288219 \leq \mathscr{C}_1 \leq 0.5409288220. \tag{2.0.1}$$

The case $p = 1$ has in fact been studied by several other authors (e.g. [6, 7, 8]) since Hörmander and Bernhardsson published their paper, mainly due to $\mathscr{C}_1$'s use in problems in analytic number theory. However, the estimates produced in [3] remain the best one yet. In fact, the authors seem to not be aware of the results of Hörmander and Bernhardsson, almost as if they were forgotten. As an example, in [8, Extremal Problem 1], it is clear that the constant $\mathcal{C}(\infty)$ is equal to $2\mathscr{C}_1$, but there is no mention of the work of Hörmander and Bernhardsson. In addition, the bounds produced in [8] correspond to

$$0.540925\ldots \leq \mathscr{C}_1 \leq 0.548845\ldots,$$

which is considerably worse than (2.0.1), at least from above. Therefore it is of great interest to study whether the techniques of Hörmander and Bernhardsson yield estimates similar to (2.0.1) for the cases $1 < p < 2$.

In the other tail-end of our interval for p, we have the special Hilbert space PW^2, where it has been proven that $\mathscr{C}_2 = 1$. In fact this is the only known value for $\mathscr{C}_p$. This is due to the fact that for all f in PW^2, we have the following reproducing kernel [1];

$$f(0) = \int_{-\infty}^{\infty} f(x) \operatorname{sinc} \pi x dx,$$

where we use the unnormalized version of the sinc function

$$\operatorname{sinc} x \coloneqq \frac{\sin x}{x}.$$

For $p \neq 2$, the exact reproducing kernels for functions in PW^p have not yet been identified. Hörmander and Bernhardsson had hoped to be able to identify their extremal from the numerical data, but were unable to do so.

CHAPTER

THREE

METHODS

3.1 Formulating an ansatz function

To approach the problem of estimating $\mathscr{C}_p$, we will start with expressing $\mathscr{C}_p$ as the solution to the following extremal problem;

$$\frac{1}{\mathscr{C}_p} = \inf_{f \in PW^p} \left\{ ||f||_p^p : f(0) = 1 \right\}. \tag{3.1.1}$$

Via a compactness argument and a rescaling argument, one can show that (3.1.1) admits a solution for any $p \in (0, \infty)$ [1], and that these extremal functions are of type exactly π. Strict convexity of L^p for $1 < p < \infty$ implies the extremal is unique, but we are "only" interested in the range $1 < p < 2$. Hörmander was made aware by Professor Helmut Rüssmann that, for $\mathscr{C}_1$, the function

$$f_1(x) = \frac{3 \sin \pi x - 3\pi x \cos \pi x}{\pi^3 x^3}$$

was close to the unique extremal function, and was able to approximate the extremal via a perturbation of this ansatz function. As previously stated, $\mathscr{C}_2 = 1$ is the only known value for $\mathscr{C}_p$, with $f_2(x) = \operatorname{sinc} \pi x$ being the extremal function in this case. By examining both f_1 and f_2, the hypothesis in [1] is that the function

$$f_p(x) = \frac{2}{B(1/2, 2/p)} \int_{-\pi}^{\pi} \left(1 - \frac{\xi^2}{\pi^2}\right)^{\frac{2}{p}-1} e^{ix\xi} d\xi/2\pi \tag{3.1.2}$$

is close to the exact extremal function, in the sense that $||f_p||_p^{-p}$ is close to $\mathscr{C}_p$. Here we denote by $B(\cdot, \cdot)$ the beta function, which is defined by

$$B(x, y) = \int_0^1 t^{x-1}(1-t)^{y-1} dt, \quad \Re x, \Re y > 0. \tag{3.1.3}$$

The beta function is closely related to the gamma function, and it can be shown that

$$B(x, y) = \frac{\Gamma(x)\Gamma(y)}{\Gamma(x+y)}.$$

A proof of this relation is given in Appendix A. To see that $\operatorname{sinc}\pi x$ actually is equal to (3.1.2) for $p = 2$, we recall that it is the inverse Fourier transform of the rectangular box, that is the function

$$\Pi(x) = \begin{cases} 1, & |x| \leq \pi \\ 0, & |x| > \pi \end{cases} = 1\chi_{[-\pi,\pi]},$$

where χ_A is the well-known indicator function. Thus it is clear that $\operatorname{sinc}\pi x = f_2(x)$. By examining the Fourier transform of f_1, we see that the same holds when $p = 1$. These f_p's can all be written in either the form of Bessel functions modified by division with a power of x, or in the form of confluent hypergeometric functions. This will prove to be a useful tool for the numerical calculations.

3.2 Different representations of f_p

In this section we will discover some other ways to represent f_p. As stated previously, f_p can be written in the form of either a Bessel function, or a confluent hypergeometric function. A useful tool is the relation

$$ {}_0F_1(a+1; -\frac{x^2}{4}) = 2^a\Gamma(a+1)x^{-a}J_a(x), \tag{3.2.1}$$

for any a and any x for which ${}_0F_1$ and J_a are well-defined. The confluent hypergeometric limit function is defined as follows;

$$ {}_0F_1(a; z) = \sum_{n=0}^{\infty} \frac{z^n}{(a)_n n!},$$

where $(a)_n$ is the Pochhammer symbol, also called the rising factorial, and is defined as $\Gamma(a+n)/\Gamma(a)$. We also have the following integral representation of ${}_0F_1$;

$$ {}_0F_1(b; z) = \frac{\Gamma(b)}{\sqrt{\pi}\Gamma(b-1/2)} \int_{-1}^{1} \left(1-t^2\right)^{b-3/2} e^{-2t\sqrt{z}} dt, \quad \Re(b) > 1/2.$$

We can already see a road to finding a representation of f_p by way of ${}_0F_1$. By setting $b - 3/2 = 2/p - 1$, we can see that

$$\begin{aligned} b - \frac{3}{2} &= \frac{2}{p} - 1 \\ \implies b &= \frac{2}{p} + \frac{1}{2}, \end{aligned}$$

and since $1 < p < 2$, we can assure that $\Re(b) > 1/2$. We then turn to the fraction in front of the integral. Now that $b = 2/p + 1/2$, we can see that

$$\frac{\Gamma(b)}{\sqrt{\pi}\Gamma(b-1/2)} = \frac{\Gamma(2/p+1/2)}{\Gamma(1/2)\Gamma(2/p)} = \frac{1}{B(1/2, 2/p)},$$

since $\Gamma(1/2) = \sqrt{\pi}$. By evaluating in $z = -\pi^2x^2/4$, and using the u-substitution $\tau = -\pi t$, we see that in fact

$$ f_p(x) = {}_0F_1(\frac{2}{p} + \frac{1}{2}; -\frac{\pi^2x^2}{4}). \tag{3.2.2}$$

Then by the main relation between ${}_0F_1$ and the Bessel functions, we must also have

$$f_p(x) = 2^{2/p-1/2}\Gamma(2/p+1/2)(\pi x)^{1/2-2/p}J_{2/p-1/2}(\pi x).$$

These representations will be vital in formulating the numerical scheme for the extremal problem in (3.1.1), as defining functions by their Fourier integral numerically leads to high computational complexity. Instead, we can use already implemented functions within Python libraries such as SciPy or mpmath.

3.3 The main inequality

It is clear that any function f in PW^p, with $f(0) = 1$, will yield a lower bound for $\mathscr{C}_p$, via taking the reciprocal of its L^p integral. But we still need some control over the upper bound of $\mathscr{C}_p$. We will make use of a result from [1, Theorem 3.10], which states that for any function $\varphi \in PW^p$ which evaluates to 1 in the origin

$$\frac{1}{||\varphi||_p} \leq \mathscr{C}_p^{1/p} \leq \frac{1}{||\varphi||_p} + ||\varphi_2 - \Phi * \varphi_2||_q, \tag{3.3.1}$$

where p and q are conjugate exponents. The function φ_2 is simply $\operatorname{sinc} \pi x$, whereas

$$\Phi(x) \coloneqq \frac{|\varphi(x)|^{p-2}\varphi(x)}{||\varphi||_p^p}. \tag{3.3.2}$$

The lower bound is trivial, as any function in PW^p naturally has to obey this given how $\mathscr{C}_p$ is defined in (3.1.1). The proof in [1] is not hard to follow, but I will nevertheless give a version of it here.

First we define $F \coloneqq \varphi_2 + \Phi - \Phi * \varphi_2$, and then take its convolution with an arbitrary f in the intersection of the Schwartz class, denoted by $\mathscr{S}$, and PW^2. Recall that, for any $f \in PW^2$, sinc is a reproducing kernel, so point evaluation is simply convolution with $\operatorname{sinc} \pi x$. Thus $\varphi_2 * f = f$. We then have that

$$F * f = \varphi_2 * f + \Phi * f - (\Phi * \varphi_2) * f$$

by distributivity of convolution. By associativity of convolution, we must then have

$$F * f = f + \Phi * f - \Phi * (\varphi_2 * f) = f + \Phi * f - \Phi * f = f.$$

This means that F is a reproducing kernel for f, i.e.

$$\begin{aligned} f(0) &= \int_{-\infty}^{\infty} F(x)f(x)dx \\ \implies |f(0)| &\leq ||Ff||_1 \leq ||F||_q||f||_p, \end{aligned}$$

where the last inequality holds by Hölder's inequality. Taking the L^p integral of f is not a problem, since $\mathscr{S}$ is dense in all L^p spaces when $1 \leq p < \infty$, and f must therefore be L^p-integrable. By rearranging the inequality, we have

$$\frac{|f(0)|}{||f||_p} \leq ||F||_q,$$

but recall that $\mathscr{C}_p^{1/p}$ is the supremum of the left hand side, so necessarily

$$\mathscr{C}_p^{1/p} \leq ||F||_q.$$

What is left now is examining the L^q integral of F. From the triangle inequality it is clear that

$$||F||_q \leq ||\Phi||_q + ||\varphi_2 - \Phi * \varphi_2||_q,$$

and so we must calculate $\|\Phi\|_q^q$. We know that

$$\|\Phi\|_q^q = \|\varphi\|_p^{-pq} \int_{\mathbb{R}} \left||\varphi|^{p-2}\varphi\right|^q dx,$$

and since p and q are conjugate exponents we must have

$$p^{-1} + q^{-1} = 1 \implies p + q = pq \implies p = q(p-1).$$

Therefore we can show that

$$\begin{aligned}
\|\Phi\|_q^q &= \|\varphi\|_p^{-pq} \int_{\mathbb{R}} \left||\varphi|^{p-2}\varphi\right|^q dx \\
&= \|\varphi\|_p^{-pq} \int_{\mathbb{R}} |\varphi|^{(p-2+1)q} dx \\
&= \|\varphi\|_p^{-pq} \int_{\mathbb{R}} |\varphi|^p dx \\
&= \|\varphi\|_p^{p-pq} = \|\varphi\|_p^{-q}.
\end{aligned}$$

The right hand side of (3.3.1) then follows by density of $\mathscr{S}$.

Since, in our case, $1 < p < 2$, we can use the Hausdorff–Young inequality to produce a weaker, but hopefully more numerically manageable inequality than (3.3.1). Recall that the Hausdorff–Young inequality states the following;

Theorem 3.3.1 (Hausdorff–Young)**.** *Let $f \in L^p(\mathbb{R})$, where $1 \leq p \leq 2$. Then*

$$||\widehat{f}||_q \leq ||f||_p, \quad \frac{1}{p} + \frac{1}{q} = 1. \tag{3.3.3}$$

We have already seen that $\Phi \in L^q$, and it is a well-known fact that $\varphi_2 \in L^r$ for any $r > 1$. Thus it is of interest to compute the inverse Fourier transform of $\varphi_2 - \Phi * \varphi_2$. Since the sinc function is even, it is clear that

$$\widecheck{\varphi_2} = \frac{1}{2\pi}\widehat{\varphi_2} = \frac{1}{2\pi}\chi_{[-\pi,\pi]}.$$

Since Φ is even as well, we get by a similar argument

$$\widecheck{\Phi * \varphi_2} = \frac{1}{2\pi}\widehat{\Phi}\chi_{[-\pi,\pi]}.$$

Therefore, by Hausdorff–Young,

$$||\varphi_2 - \Phi * \varphi_2||_q \leq \left(\int_{-\pi}^{\pi} \left|1 - \widehat{\Phi}(\xi)\right|^p \frac{d\xi}{2\pi}\right)^{1/p}. \tag{3.3.4}$$

By examining the right-hand side it seems that, for non-integer p's, this could prove to be a nightmare to compute numerically. Therefore it is of interest to look for some way to simplify our numerical task. This will of course yield a suboptimal bound, but it may be better than nothing at all. Note that in (3.3.4), the right-hand side is simply

$$(2\pi)^{-1/p}|| \left(1 - \widehat{\Phi}\right) \chi_{[-\pi,\pi]}||_p.$$

By the Hölder inequality, we have that

$$||fg||_p \leq ||f||_2||g||_q, \quad \frac{1}{p} = \frac{1}{q} + \frac{1}{2},$$

for suitable functions f and g. In our case, we define

$$\begin{aligned} f(\xi) &= \left(1 - \widehat{\Phi}\right) \chi_{[-\pi,\pi]} \\ g(\xi) &= 1\chi_{[-\pi,\pi]}, \end{aligned}$$

and thus we have that

$$\begin{aligned} ||fg||_p \leq ||f||_2||g||_q &= (2\pi)^{1/p-1/2} \, ||f||_2 \\ \implies (2\pi)^{-1/p} \, ||f||_p &\leq (2\pi)^{-1/2} \, ||f||_2, \end{aligned} \tag{3.3.5}$$

which means that

$$||\varphi_2 - \Phi * \varphi_2||_q \leq \left(\int_{-\pi}^{\pi} \left|1 - \widehat{\Phi}\right|^2 \frac{d\xi}{2\pi} \right)^{1/2}. \tag{3.3.6}$$

Notice that we can utilise Parseval's identity now, and recall that it states that

$$||f||_{L^2(-\pi,\pi)} = \left(2\pi \sum_{n=-\infty}^{\infty} |c_n|^2 \right)^{1/2}, \quad c_n = \frac{1}{2\pi} \int_{-\pi}^{\pi} f(x) e^{-inx} dx. \tag{3.3.7}$$

Therefore our task reduces to computing the Fourier coefficients of the function

$$1 - \widehat{\Phi}(\xi).$$

The Fourier coefficients of the function $\xi \mapsto 1$ are trivial, as we have

$$\frac{1}{2\pi} \int_{-\pi}^{\pi} e^{-inx} dx = \operatorname{sinc} \pi n,$$

which equals 1 when $n = 0$, and 0 for every other $n \in \mathbb{Z}$. Thus we have some candidates for estimating the upper bounds for $\mathscr{C}_p$.

3.4 An extremal problem in L^p

The first, and most approachable, obstacle is to improve the lower bound for $\mathscr{C}_p$ via solving the extremal problem in (3.1.1) numerically. This will not give us an exact extremal, but the hope is that it will yield a function "close enough" to

the actual extremal, although it seems unlikely that we will reach the accuracy of Hörmander and Bernhardsson. In their paper, Hörmander's approach was to consider the integral

$$I_p(\varepsilon) = \int_0^\infty |G + \varepsilon H|^p \, dx,$$

where $G = f_1$, and H is a perturbation of f_1, which must have the property $H(0) = 0$ and $\widehat{H}(\pm\pi) = 0$. Recall that Hörmander studied the case $p = 1$ only. He realised that f_1 was equal to the inverse Fourier transform of $(1-\xi^2/\pi^2)\chi_{[-\pi,\pi]}$, up to a constant. He does not explicitly state this in his and Bernhardsson's paper, but we are led to believe he considered the following basis for his perturbation of f_1;

$$\begin{aligned} \varepsilon H(x) &= \sum_k c_k H_k, \quad k = 1, 2, \cdots \\ \widehat{H_k}(\xi) &= \left[A\left(1 - \frac{\xi^2}{\pi^2}\right)^{k+1} - B\left(1 - \frac{\xi^2}{\pi^2}\right)^{k} \right] \chi_{[-\pi,\pi]}, \end{aligned} \tag{3.4.1}$$

where A and B are some constants so that $H_k(0) = 0$ for all k. This was covered in the project thesis [5, Section 4].

In the case of $1 < p < 2$, our aim was to modify this approach to find a minimizer for I_p. Notice that we are only integrating over $\mathbb{R}^+$, because the extremal function must necessarily be even [1]. Thus when I_p has been minimized (numerically), we have the following lower bound for $\mathscr{C}_p$;

$$\frac{1}{2I_p(c_{ex})} \leq \mathscr{C}_p, \tag{3.4.2}$$

where c_{ex} is the minimizer. Our initial function is of course f_p, as defined in (3.1.2). One can clearly see that its Fourier transform is

$$\widehat{f_p}(\xi) = \frac{2}{B(1/2, 2/p)} \left(1 - \frac{\xi^2}{\pi^2}\right)^{2/p-1} \chi_{[-\pi,\pi]}.$$

Following in Hörmander's footsteps, it would seem natural to consider a basis of functions of similar form to (3.4.1), with the modification that we are now looking at the Fourier transforms being of form

$$\left[A\left(1 - \frac{\xi^2}{\pi^2}\right)^{(2/p-1)(k+1)} - B\left(1 - \frac{\xi^2}{\pi^2}\right)^{(2/p-1)k} \right] \chi_{[-\pi,\pi]}.$$

It is though important to realise we have to be careful when determining the constants A & B, as they clearly must depend on p. Recalling the beta function, notice that

$$\begin{aligned} B(1/2, y) &= \int_0^1 t^{-1/2}(1-t)^{y-1} dt \\ &= 2\int_0^1 (1-s^2)^{y-1} ds \\ &= \int_{-1}^1 (1-s^2)^{y-1} ds \\ &= 2\int_{-\pi}^{\pi} \left(1 - \frac{\xi^2}{\pi^2}\right)^{y-1} \frac{d\xi}{2\pi}. \end{aligned}$$

This means that when $y = (2/p-1)k+1$, we have

$$\frac{B(1/2, k(2/p-1)+1)}{2} = \int_{-\pi}^{\pi} \left(1 - \frac{\xi^2}{\pi^2}\right)^{k(2/p-1)} \frac{d\xi}{2\pi}.$$

Thus the reciprocal of the left side is the normalization factor chosen such that each basis function evaluates to 0 in the origin.

Let us define $d_{k,p}$ and $h_{k,p}$ as follows:

$$d_{k,p}(x) \coloneqq \frac{2}{B(1/2, k(2/p-1)+1)} \int_{-\pi}^{\pi} \left(1 - \frac{\xi^2}{\pi^2}\right)^{k(2/p-1)} e^{ix\xi} \frac{d\xi}{2\pi}, \tag{3.4.3}$$

$$h_{k,p}(x) \coloneqq d_{k+1,p}(x) - d_{k,p}(x). \tag{3.4.4}$$

Thus we end up with the following integral to be minimized;

$$I_p(c) = \int_0^{\infty} \left| f_p(x) + \sum_k c_k h_{k,p}(x) \right|^p dx. \tag{3.4.5}$$

Let us, for ease of notation going forward, denote $h(x) \coloneqq \sum_k c_k h_{k,p}(x)$. Using the representation found in the previous section, we can also see that

$$d_{k,p}(x) = {}_0F_1\left(k\left(\frac{2}{p} - 1\right) + \frac{3}{2}; -\frac{\pi^2 x^2}{4}\right).$$

In [3] the integral $I_1(\varepsilon)$ was minimized by using Newton's method. Therefore it seemed feasible that this approach could be used for minimizing I_p for $1 < p < 2$. Recall that the multivariate Newton–Raphson method for minimizing a function F is defined as follows

$$x_{n+1} = x_n - \left[\nabla^2 F(x_n)\right]^{-1} \cdot \nabla F(x_n)$$

with an initial guess x_0. Thus we need to study the derivatives of $I_p(c)$. The first derivatives of I_p with respect to the c_k's are as follows

$$\begin{aligned} \frac{\partial I_p(c)}{\partial c_j} &= \int_0^{\infty} \partial_{c_j} |f_p + h|^p \, dx \\ &= \int_0^{\infty} p \, |f_p + h|^{p-1} \frac{f_p + h}{|f_p + h|} h_{j,p}(x) dx \\ &= \int_0^{\infty} p \, |f_p + h|^{p-2} (f_p + h) \, h_{j,p}(x) dx. \end{aligned} \tag{3.4.6}$$

We may differentiate under the integral sign without worry, as by [1, Lemma 3.2(a)] the extremal φ_p has simple zeros for $p \geq 1/2$, and it is a known result for Bessel functions that

$$x^{-a} J_a(x)$$

has simple zeros.

The second derivatives are somewhat more troublesome. We note that in the second integral, the integrand contains

$$\frac{f_p + h}{|f_p + h|} \equiv \operatorname{sgn}(f_p + h).$$

We will also keep in mind that

$$\left(\frac{f_p + h}{|f_p + h|}\right)^2 (x) = 1 \quad \text{a.e..}$$

It evaluates to 0 at the zeros of $f_p(x) + h(x)$, but the integrals do not see sets of measure zero, and since the zeros of $f_p + h$ are simple, we do not arrive at any problems.

Hörmander exploited this for $p = 1$, where the integrand in the first derivative simply becomes $\operatorname{sgn}(f + h)h_{j,1}$. This simplified their calculation of the second derivatives, as this reduced to a summation of the terms

$$2(-1)^n \frac{h_{j,1}(t_n)h_{i,1}(t_n)}{(f_1 + h)'(t_n)},$$

where $(t_n)_{n\in\mathbb{N}}$ were the positive zeros of $f_1 + h$. This is not the case for $p \neq 1$. Nevertheless, we can still derive the second derivatives of I_p;

$$\begin{aligned} \left(\nabla^2 I(c)\right)_{ij} &= \frac{\partial}{\partial c_i} \int_0^\infty p\,|f_p + h|^{p-2}\,(f_p + h)\,h_j dx \\ &= p \int_0^\infty h_j \partial_i \left[|f_p + h|^{p-2}\,(f_p + h)\right] dx, \end{aligned} \tag{3.4.7}$$

where we need to study the integrand further. Differentiating the left term in the integrand with respect to c_i yields

$$\begin{aligned} (f_p + h)\,\partial_i |f_p + h|^{p-2} &= (p-2)|f_p + h|^{p-3} \frac{f_p + h}{|f_p + h|}(f_p + h)h_i \\ &= (p-2)|f_p + h|^{p-2} \left(\frac{f_p + h}{|f_p + h|}\right)^2 h_i \\ &= (p-2)|f_p + h|^{p-2} h_i, \end{aligned}$$

whereas differentiating the right term yields

$$|f_p + h|^{p-2}\,\partial_i (f_p + h) = |f_p + h|^{p-2}\,h_i.$$

Thus by differentiating the whole integrand using the product rule, we get

$$\left(\nabla^2 I(c)\right)_{ij} = p(p-1) \int_0^\infty |f_p + h|^{p-2}\,h_i h_j dx. \tag{3.4.8}$$

Having derived the expressions for both the gradient and the Hessian matrix, we can solve the extremal problem numerically in Python. This was done using the Python library mpmath, along with the module gmpy2, which allows for arbitrary precision floating-point arithmetic. This library was favored ahead of SciPy and NumPy, as these libraries seemed to poorly handle the oscillatory nature of the integrands.

3.5 Remarks on $p = 1$

The case of $p = 1$ is a curious one. Recall that when φ is the extremal, (3.3.2) gives rise to a reproducing kernel, which in the case of $p = 1$ is

$$\Phi(x) = \frac{\operatorname{sgn} \varphi(x)}{||\varphi||_1}.$$

Examining the initial function f_1, Hörmander made great use of the fact that $u = \operatorname{sgn} f_1$ behaved similarly to

$$x \mapsto -\operatorname{sgn} \cos \pi x, \tag{3.5.1}$$

which changes sign at the half-integers. He also noticed that the positive zeros of f_1 lay close to $a_n = n + \frac{1}{2}$, $n = 1, 2, \ldots$, which of course are the positive zeros of $\cos \pi x$ larger than $\frac{1}{2}$. Since both f_1 and $\cos \pi x$ are even functions, their signs must be too, and so we need only examine them on the positive real line. Using this relation, Hörmander was able to, rather miraculously, gain a very tight upper bound for $\mathscr{C}_1$. It is known that the Fourier transform of a P-periodic signal f is, in the distributional sense,

$$\begin{aligned} \widehat{f}(\xi) &= 2\pi \sum_{n=-\infty}^{\infty} c_n \delta(\frac{2\pi n}{P} - \xi) \\ c_n &= \frac{1}{P} \int_P f(x) e^{-i2\pi \frac{n}{P} x} dx, \end{aligned} \tag{3.5.2}$$

where $\delta(x)$ is the usual delta measure on $\mathbb{R}$. (3.5.1) is 2-periodic with mean value 0, so its Fourier transform simply consists of point masses at $\xi = n\pi$, with the weights being equal to $2\pi c_n$. The fact that u exhibited said behaviour, allowed Hörmander to express the Fourier transform of u as

$$\widehat{u}(\xi) = 4 \sum_{k=0}^{\infty} (-1)^k \int_{t_k}^{a_k} \cos \pi x \xi dx, \tag{3.5.3}$$

where t_k were the zeros of f_1 [3, Equation 3.10]. It is not as simple for $1 < p < 2$, as Φ is not a simple sign-function. Should one, however, examine Φ as $p \to 1$, it seems to continually deform from $\operatorname{sinc} \pi x$ into $\operatorname{sgn} f_p$.

The expression in (3.5.3) leads to a tighter inequality than the one in (3.3.1), which is the main reason why the bounds for $\mathscr{C}_1$ are so precise. Another point of interest is how the integrands in the derivatives of I_p changes as $p \to 1$, as previously mentioned. This reduced the numerical complexity significantly, as instead of integrating a highly oscillatory function, the calculation reduced to a summation over the zeros of $f_1 + h$.

3.6 An upper estimate for $\mathscr{C}_p$

To gain an upper bound for $\mathscr{C}_p$, and to show it is not much larger than the lower bounds found via Newton's method, we need to estimate the right hand side of (3.3.1). Hörmander and Bernhardsson made use of the fact that for $p = 1$

$$\Phi(x) = \frac{\operatorname{sgn} \varphi}{||\varphi||_1}(x),$$

which made the calculation of (3.3.4) significantly easier, since this function behaves similarly to $-\operatorname{sgn}\cos \pi x$. This is not the case for other p's, as

$$\Phi(x) = \frac{|\varphi|^{p-1} \operatorname{sgn} \varphi(x)}{||\varphi||_p^p},$$

and calculating the integral in (3.3.4) is a difficult numerical task. After some difficulties with computing the Fourier coefficients of (3.3.2), we decided to numerically approximate the convolution

$$\Phi * \varphi_2,$$

by using the built in function `convolve` from `scipy.signal`. This functions samples the two functions on some finite interval, and produces a numerical approximation of the convolution on this interval. To ensure the convolution was accurate on this interval, it was important to have enough sample points, to be able to effectively capture the oscillating nature of both functions. Therefore we chose to use $10^3 N + 1$ equidistant sample points for the interval $(-N, N)$, which is equivalent to a sample rate of 500, i.e. 500 samples per unit length. Since both $\operatorname{sinc} \pi x$ and Φ decay relatively fast, it is reasonable to assume the main contribution to the L^q norm is contained in the interval $(-10^4, 10^4)$. Then, after producing this convolution, we turn to approximating the L^q norm in (3.3.1). To approximate this L^q norm, we will integrate the samples using `np.trapz`, which approximates the integral of the function using the trapezoidal rule, which is a 2^{nd} order numerical integration technique.

This will, of course, yield some numerical error. In the first instance, we are sampling the functions over a finite interval, and then integrating using the sample points, so we will need to estimate the contribution from the tail-ends of the integral. In other words, we need to find an estimate for

$$\int_{|x|>10000} |\varphi_2 - \Phi * \varphi_2|^q \, dx. \tag{3.6.1}$$

CHAPTER

FOUR

RESULTS

4.1 Lower bounds for $\mathscr{C}_p$

The lower bounds arising from (3.4.2) are presented in Table 4.1.1, while the lower bound arising from the ansatz functions, f_p, are presented in Table 4.1.2.

p	**c**	$\mathscr{C}_p \geq$
1	0.029854	0.5409288219
1.1	0.026205	0.5904496737
1.2	0.020401	0.6390809499
4/3	0.014428	0.7026277974
1.4	0.011869	0.7338627545
1.5	0.008446	0.7800570531
1.7	0.002707	0.8701760940
1.8	-0.000440	0.9141453879
2	0.000000	1

Table 4.1.1: Lower bounds for $\mathscr{C}_p$ after Newton iteration. The parameter **c** denotes the minimizer in (3.4.5).

This shows that the Newton iteration yields stronger lower bounds for $\mathscr{C}_p$, as we had hoped. It is also evident that we are making a similar improvement in the lower bound as Hörmander and Bernhardsson did in [3], as we seem to improve the lower bounds in the 5^{th} decimal place for the different values of p.

4.2 Upper bounds for $\mathscr{C}_p$

The upper bounds were found by numerically estimating the rightmost term in (3.3.1), and adding this to the lower bounds in Table 4.1.1, and are presented in

p	$\mathscr{C}_p \geq$
1	0.5408879784
1.1	0.5903918196
1.2	0.6390350580
4/3	0.7025916777
1.4	0.7338280575
1.5	0.7800255171
1.7	0.8701452647
1.8	0.9141164376
2	1

Table 4.1.2: Lower bounds for $\mathscr{C}_p$ before Newton iteration, acquired by calculating $\|f_p\|^{-1}$.

Table 4.2.1. It is clear by the table values that our numerical computation does not yield particularly tight upper bounds, especially for p's closer to $p = 1$. An important disclaimer is that we cannot be 100% certain that these upper bounds are correct, as we need to study the numerical error in the convolution algorithm. Therefore these estimates must, in the first place, rather be understood as evidence supporting the claim that the upper bounds are not much larger than the lower bounds in Table 4.1.1.

p	$\mathscr{C}_p \leq$
1	0.5409288220
1.1	0.8111373925
1.2	0.7265669010
4/3	0.7411531953
1.4	0.7613370212
1.5	0.7976297081
1.7	0.8786150672
1.8	0.9203609850
2	1

Table 4.2.1: Upper bounds arising from numerical convolution.

4.3 A plot of the upper and lower bounds for $\mathscr{C}_p$

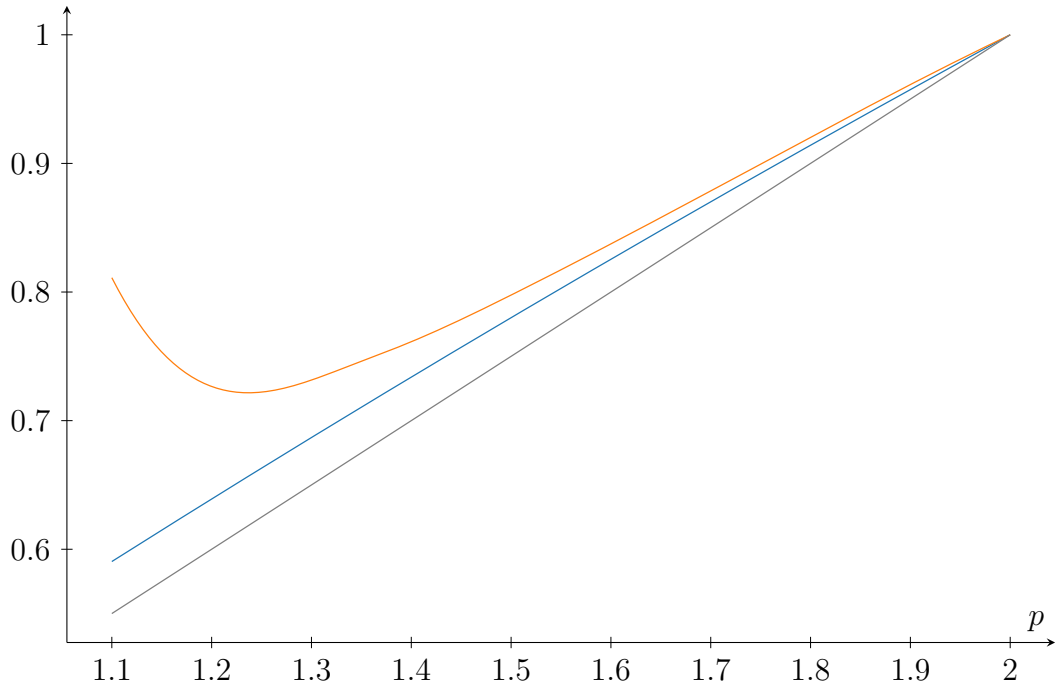

Figure 4.3.1: Upper and lower bounds for $\mathscr{C}_p$, as functions of p. The curve $p/2$ is included as a reference curve.

The plot in Figure 4.3.1 shows that our upper and lower bounds are very tight for values of p close to 2, but the two curves seem to diverge from each other as $p \searrow 1$. It was mentioned in [1] that for $p = 1$, the functional

$$\varphi_2 - \Phi * \varphi_2$$

may be unbounded on the space $\mathscr{S} \cap L^1(\mathbb{R})$, in the sense that we have no control over

$$\|\varphi_2 - \Phi * \varphi_2\|_\infty.$$

Should this be true, it would make sense that the orange curve in Figure 4.3.1 would begin to grow rapidly towards $+\infty$ as $p \searrow 1$. Unfortunately we have not managed to prove, or disprove, this hypothesis.

4.4 Upper and lower bounds together

Combining the lower and upper bounds for $\mathscr{C}_p$ for the samples in Table 4.1.1 and Table 4.2.1, we write out the following inequalities;

$$0.5904496737 \leq \mathscr{C}_{1.1} \leq 0.8111373925, \tag{4.4.1}$$

$$0.6390809499 \leq \mathscr{C}_{1.2} \leq 0.7265669010, \tag{4.4.2}$$

$$0.7026277974 \leq \mathscr{C}_{4/3} \leq 0.7411531953, \tag{4.4.3}$$

$$0.7338627545 \leq \mathscr{C}_{1.4} \leq 0.7613370212, \tag{4.4.4}$$

$$0.7800570531 \leq \mathscr{C}_{1.5} \leq 0.7976297081, \tag{4.4.5}$$

$$0.8701760940 \leq \mathscr{C}_{1.7} \leq 0.8786150672, \tag{4.4.6}$$

$$0.9141453879 \leq \mathscr{C}_{1.8} \leq 0.9203609850. \tag{4.4.7}$$

4.5 The case $p = 4/3$

The case $p = 4/3$ is another curious case. A big thank you to PhD-student Sarah May Instanes who made us aware of an interesting result for the upper bound of $\mathscr{C}_{4/3}$ [9],

$$\mathscr{C}_{4/3} < 0.713.$$

This result came from considering the approach from [1, Section 6], and realizing that the intervals on level $n+3$ are copies of the intervals on level n, which gave the following bound for $\mathscr{C}_{4/3}$;

$$\mathscr{C}_{4/3} \leq 2\int_0^{\frac{5}{4}} \frac{\sin^2 \frac{2}{3}\pi x}{\pi^2 x^2} dx + 2\sum_{n=1}^{\infty} \int_{n+\frac{1}{4}}^{n+\frac{5}{4}} \frac{\sin^2 \frac{2}{3}\pi (x-n)}{\pi^2 x^2} dx < 0.713. \tag{4.5.1}$$

This is evidently a stronger bound than the upper bound we found via the numerical convolution, but it seems difficult to replicate this for other $1 < p < 2$.

4.6 Error analysis

Since the rightmost term in (3.3.1) is estimated numerically, we need to estimate the error in this calculation. First we need to estimate what error we accumulate when numerically integrating over the interval $(-10^4, 10^4)$, and then we need to bound the integral over $\mathbb{R} \setminus (-10^4, 10^4)$.

With a sample rate of 500, the numerical convolution is sure to be very precise, as we are sampling the convolution $\Phi * \varphi_2$ on 500 points per unit length, so that we lose minimal information about the function. Then we turned to calculating the integral

$$\int_{-10^4}^{10^4} |\varphi_2 - \Phi * \varphi_2|^q \, dx \tag{4.6.1}$$

using the trapezoidal rule. The usual error bound for the composite trapezoidal rule is

$$E_{trap} \sim 1/n^2,$$

where n is the number of subintervals. This estimate gives an error $\sim 10^{-14}$. When testing against known solutions, the `np.trapz`-function seemed to exhibit an error of this magnitude. When prompting WolframAlpha to compute the integral

$$I = \int_{-10^4}^{10^4} |\operatorname{sinc} \pi x|^2 dx,$$

we got the following value for I;

$$I \simeq 0.9999898678816409\ldots.$$

While computing the same integral using `np.trapz` with $10^3 \cdot 10^4 + 1$ sample points, we got

$$I_{trap} = 0.9999898678816397,$$

which is a very accurate approximation of I, with an error in the 15^{th} decimal place. One may also notice that both I and I_{trap} are close to the actual value of $\|\operatorname{sinc} \pi x\|_2^2$, which is well known;

$$\int_{\mathbb{R}} |\operatorname{sinc} \pi x|^2 dx = 1.$$

It is also important to note that since $1 < p < 2$, we must necessarily have $2 < q < \infty$. When q is an even integer, the calculations using the trapezoidal rule exhibit errors of even lower magnitude. For example, when $q = 4$, which corresponds to $p = 4/3$, the error is $\sim 10^{-15}$. Therefore we can be confident that the numerical estimate for (4.6.1) yields a low error. The remaining part is then to give a bound for the integral

$$\left(\int_{|x|>10^4} |\varphi_2 - \Phi * \varphi_2|^q \, dx \right)^{1/q}. \tag{4.6.2}$$

When $|x| > 10^4$,

$$|\operatorname{sinc} \pi x| \leq 0.00003,$$

and $|\Phi * \varphi_2|$ will be of the same magnitude, and decaying. It is also clear that, as $|x| \to \infty$, both $\varphi_2 \to 0$ and $\Phi * \varphi_2 \to 0$. Thus we can be assured that our upper bounds for $\mathscr{C}_p$ are not much larger than the ones calculated through the numerical convolution algorithm. Plots of the convolutions versus sinc for some values of p are included in Appendix B, to illustrate how close Φ is to being a reproducing kernel for φ_2.

CHAPTER

FIVE

DISCUSSION

5.1 Discussing the results

The main observation made from the results is that the upper and lower bounds seem to get tighter as $p \nearrow 2$, which is consistent with the fact that f_p is the exact extremal when $p = 2$. The Newton–Raphson solver improved the lower bounds in roughly the same decimal places as achieved in [3], which is a positive result. This also supports the hypothesis that f_p is close to the extremal for all $1 < p < 2$, and that the upper bounds may be closer to the lower bounds than what we found in this thesis. It was also clear from the upper bounds, that the numerical convolution provided weaker upper bounds for $\mathscr{C}_p$ as $p \searrow 1$. This could be due to the fact that $\operatorname{sinc}(\pi x)$ is not L^1-integrable, and (3.3.1) must be interpreted differently when $p = 1$ compared to when $1 < p$, as the inequality must be interpreted in the distributional sense in this case.

When examining the term

$$\varphi_2 - \Phi * \varphi_2$$

for $p = 1$, it is known that $\Phi \in L^\infty$. And since φ_2 is L^2-integrable, we cannot necessarily say anything about the convolution, as convolution between L^∞ and L^2 functions is not well-defined. This is likely why the upper bound diverges from the lower bound as $p \searrow 1$, although this is unknown to us.

5.2 Numerical Difficulties

The main numerical difficulties tied to this thesis were due to the fact that we were dealing with highly oscillatory L^p-integrable functions for non-integer p's. When p is an even integer ≥ 2, taking the Fourier transform of $|f|^{p-2}f$ is handled by the Fourier convolution theorem, but this is not possible for $1 < p < 2$. Therefore the calculations ended up having a high computational complexity, which is why we used only one basis function in the Newton–Raphson implementation of the extremal problem (3.1.1). Restricting to a single basis function necessarily lead to a weaker bound for $\mathscr{C}_p$, but as covered in the project thesis [5], where we solved the extremal problem with both one and 3 basis functions, the bounds only differed in the 9^{th} decimal place, which for our purposes was sufficiently close. Estimating the upper bound also proved to be a tough numerical task, as for either of the

candidates for an upper bound, we would have to integrate over the entire real line. Because of this, we turned to sampling the functions on a sufficiently big, but finite, interval, and estimating the L^q norm of the convolution numerically.

5.3 Future work

The bounds we have furnished in this thesis are evidently not as tight as the ones Hörmander and Bernhardsson found for $\mathscr{C}_1$, so there is definitely room for improvement, on both sides of the main inequality (3.3.1).

The most obvious step further is to implement the Newton–Raphson solver with more basis functions, hopefully without the runtime skyrocketing. Hörmander and Bernhardsson's calculations were stable for 3 basis functions, and they did not gain any significant accuracy by using more than 3, so it would be reasonable to assume 3 basis functions would be enough for our case as well. It also seems likely that the machinery in (3.3.1) may not yield the tightest upper bounds for $\mathscr{C}_p$, with both the cases $p = 1$ and $p = 4/3$ supporting this claim.

Thus the main task for future work is to furnish even stronger upper bounds for $\mathscr{C}_p$, than what we have achieved, as there is definite room for improvement.

CHAPTER

SIX

CONCLUSIONS

In this master's thesis we have furnished lower bounds for $\mathscr{C}_p$ for $1 < p < 2$, and provided some calculations supporting our claim about the upper bounds for $\mathscr{C}_p$, that they are not much larger than the lower bounds we have found numerically using Newton's method. We have also found that the numerical and theoretical framework of Hörmander and Bernhardsson yields solid results for p's closer to $p = 2$, but that the upper and lower bounds from (3.3.1) seem to diverge as $p \to 1$. Lastly, we have discussed future work, and what improvements can be made to the results we have produced in this thesis.

REFERENCES

[1] O. F. Brevig, A. Chirre, J. Ortega-Cerdà, and K. Seip. "*Point Evaluation in Paley–Wiener Spaces*". In: (2022). DOI: https://doi.org/10.48550/arXiv.2210.13922.

[2] D. S. Lubinsky. "*Scaling Limits of Polynomials and Entire Functions of Exponential Type*". In: *Approximation Theory XV: San Antonio 2016*. Ed. by Gregory E. Fasshauer and Larry L. Schumaker. Cham: Springer International Publishing, 2017, pp. 219–238. ISBN: 978-3-319-59912-0.

[3] L. Hörmander and B. Bernhardsson. "*An Extension of Bohr's Inequality*". English. In: *Boundary Value Problems for Partial Differential Equations and Applications*. Ed. by Jacques Louis Lions and C. Baiocchi. France: Masson, 1993, pp. 179–194. ISBN: 9782225843341.

[4] N. B. Andersen. "*Entire Lp-functions of exponential type*". In: *Expositiones Mathematicae* 32.3 (2014), pp. 199–220. ISSN: 0723-0869. DOI: https://doi.org/10.1016/j.exmath.2013.10.003. URL: https://www.sciencedirect.com/science/article/pii/S0723086913000625.

[5] P. E. Skaug. "*On Hörmander's Extension of Bohr's Inequality*". NTNU, 2023.

[6] D. V. Gorbachev. "*An integral problem of Konyagin and the (C,L)-constants of Nikol'skii*". In: *Trudy Inst. Mat. i Mekh. UrO RAN* 11.2 (2005). *Function theory*, pp. 72–91. URL: http://mi.mathnet.ru/timm191.

[7] N. N. Andreev, S. V. Konyagin, and A. Yu. Popov. "*Extremum problems for functions with small support*". In: *Mat. Zametki* 60.3 (1996). Reprinted in: *Math. Notes*, 1996, 60(3), 241–247, https://doi.org/10.1007/BF02320360, pp. 323–332. DOI: 10.4213/mzm1833. URL: http://mi.mathnet.ru/mzm1833.

[8] E. Carneiro, M. B. Milinovich, and K. Soundararajan. "*Fourier optimization and prime gaps*". In: *Commentarii Mathematici Helvetici* 94.3 (Sept. 2019), pp. 533–568. ISSN: 1420-8946. DOI: 10.4171/cmh/467. URL: http://dx.doi.org/10.4171/CMH/467.

[9] S. M. Instanes. "*An Optimization Problem and Point Evaluation in Paley–Wiener Spaces*". in preparation. 2024.

APPENDICES

A - RELATION BETWEEN $B(\cdot,\cdot)$ AND $\Gamma(\cdot)$

The beta function is defined, for $z > 0$, as

$$\Gamma(z) = \int_0^\infty e^{-t} t^{z-1} dt, \tag{A.1}$$

and the beta function is defined as in (3.1.3). We want to prove that the following relation holds:

$$B(x,y) = \frac{\Gamma(x)\Gamma(y)}{\Gamma(x+y)}. \tag{A.2}$$

We have that

$$\begin{aligned}\Gamma(x)\Gamma(y) &= \int_0^\infty e^{-t} t^{x-1} dt \int_0^\infty e^{-\tau} \tau^{y-1} d\tau. \\ &= \int_0^\infty \int_0^\infty e^{-t-\tau} t^{x-1} \tau^{y-1} dt d\tau.\end{aligned}$$

Consider the substitutions $t = uv$ and $\tau = u(1-v)$. The Jacobian of this transformation $(t,\tau) \mapsto (u,v)$ is

$$J = \begin{vmatrix} \frac{\partial t}{\partial u} & \frac{\partial t}{\partial v} \\ \frac{\partial \tau}{\partial u} & \frac{\partial \tau}{\partial v} \end{vmatrix} = \begin{vmatrix} v & u \\ (1-v) & -u \end{vmatrix} = -u.$$

Since $u = t + \tau$ and $v = t/(t+\tau)$, the limits of integration for u are 0 to ∞, while the limits of integration for v are 0 to 1. Therefore

$$\begin{aligned}\Gamma(x)\Gamma(y) &= \int_{u=0}^\infty \int_{v=0}^1 e^{-u} (uv)^{x-1} \left(u(1-v)\right)^{y-1} u du dv \\ &= \int_{u=0}^\infty e^{-u} u^{x+y-1} du \int_{v=0}^1 v^{x-1} (1-v)^{y-1} dv \\ &= \Gamma(x+y) B(x,y).\end{aligned}$$

The result follows by dividing by $\Gamma(x+y)$ on both sides.

B - PLOTS OF CONVOLUTIONS VS. SINC

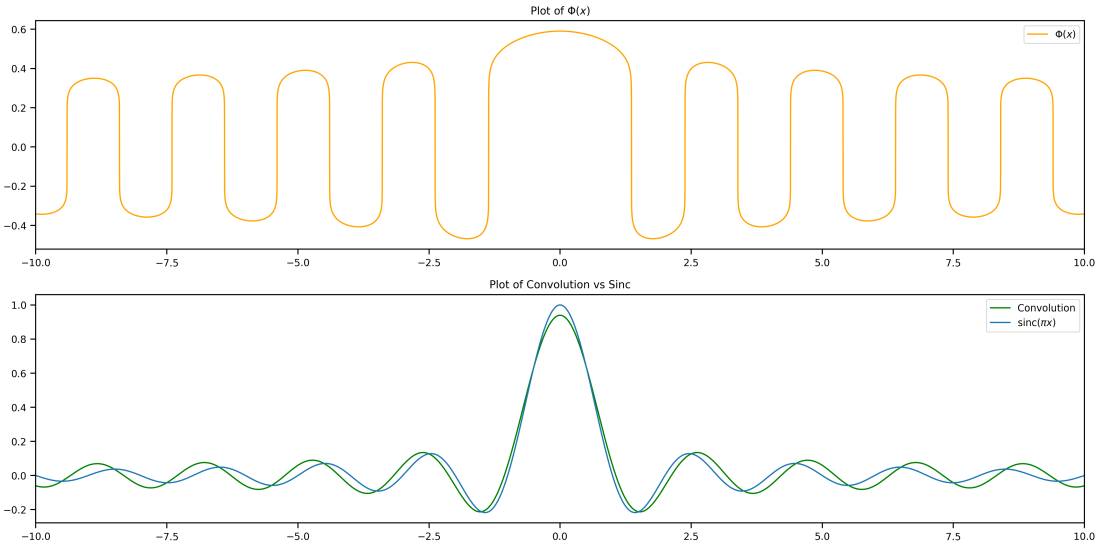

Figure B.1: Plots of $\Phi(x)$, and $\Phi * \varphi_2$ vs φ_2 when $p = 1.1$.

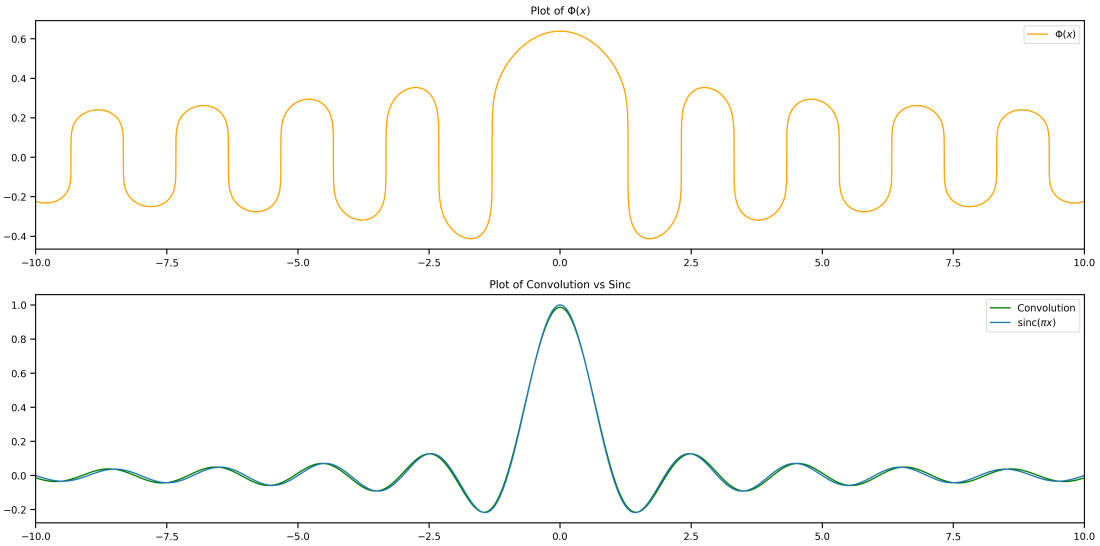

Figure B.2: Plots of $\Phi(x)$, and $\Phi * \varphi_2$ vs φ_2 when $p = 1.2$.

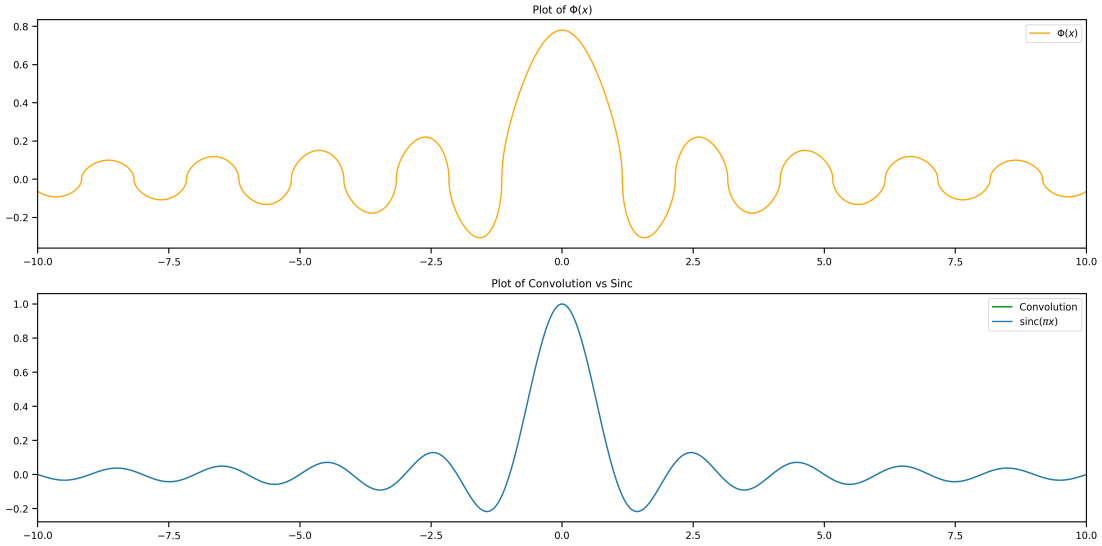

Figure B.3: Plots of $\Phi(x)$, and $\Phi * \varphi_2$ vs φ_2 when $p = 1.5$.

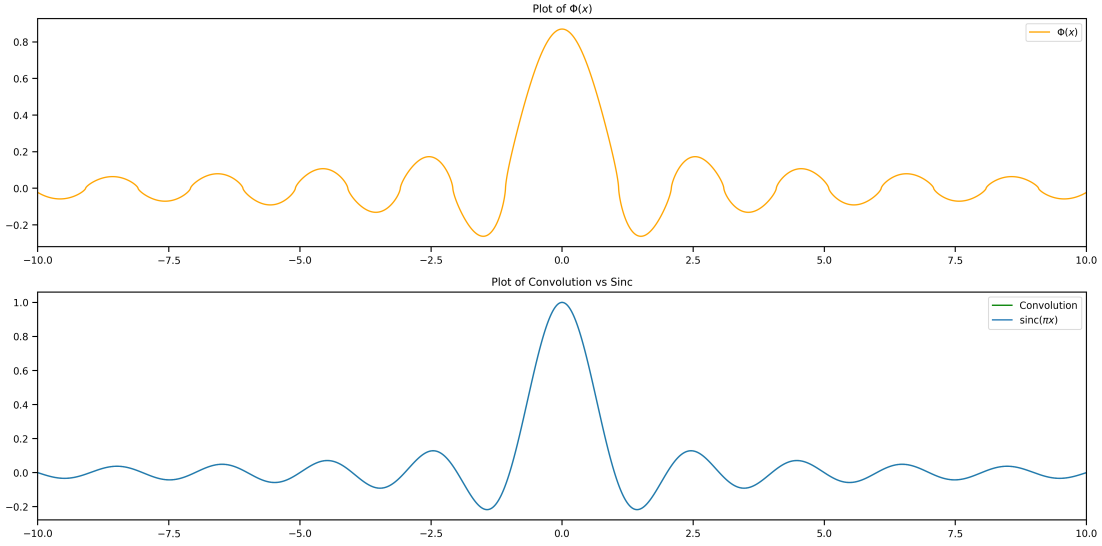

Figure B.4: Plots of $\Phi(x)$, and $\Phi * \varphi_2$ vs φ_2 when $p = 1.7$.

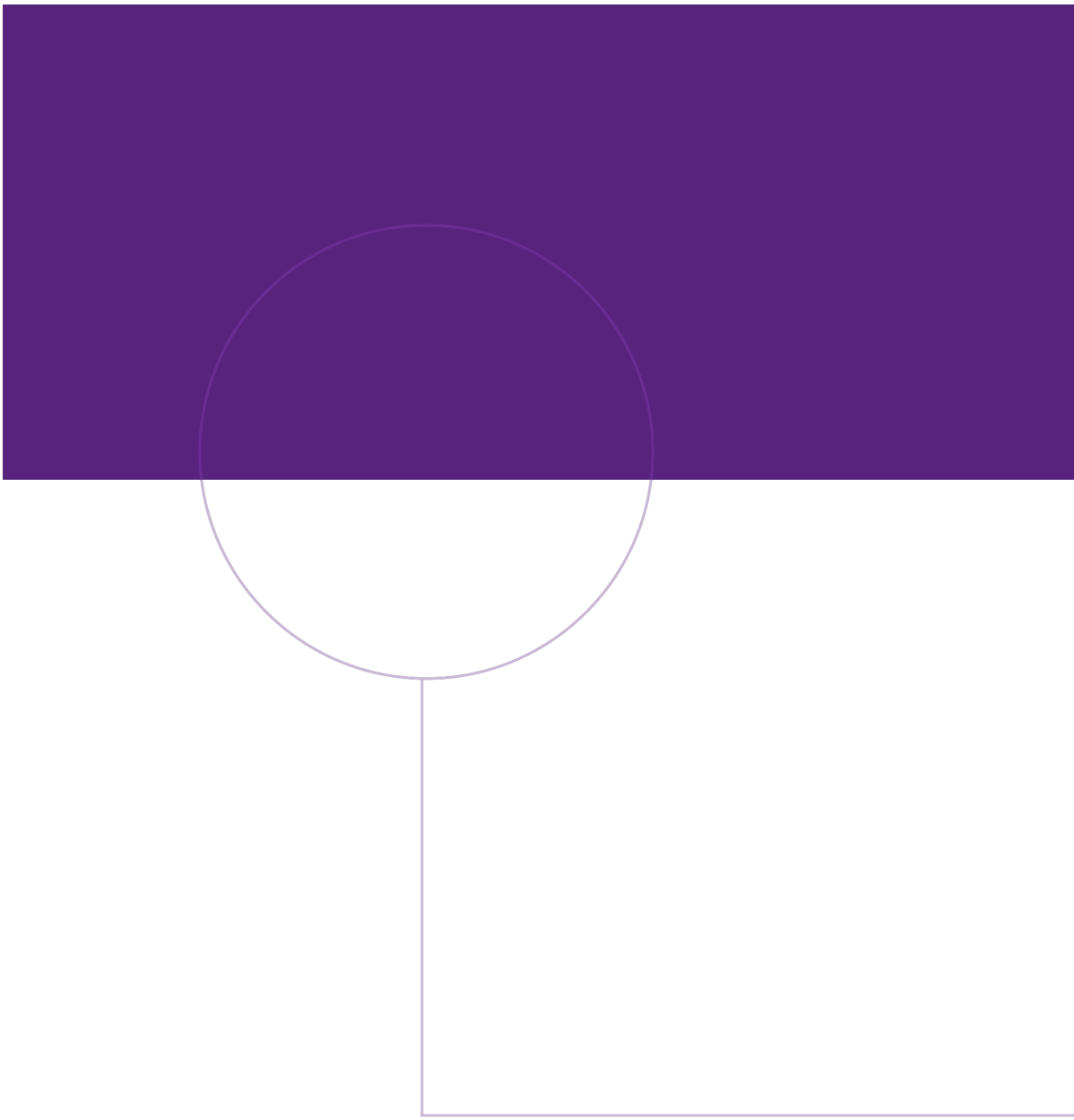

NTNU

Norwegian University of
Science and Technology